ANALYSIS OF IMMITTANCE SPECTROSCOPY DATA: MODEL COMPARISONS, UNIVERSALITY?, AND ESTIMATION OF DISTRIBUTIONS OF ACTIVATION ENERGIES

J. ROSS MACDONALD
Department of Physics and Astronomy, University of North Carolina, Chapel Hill, NC 27599, macd@gibbs.oit.unc.edu

ABSTRACT

Immittance spectroscopy [IS] involves the measurement of the small-signal frequency response of dielectrics, semiconductors, electrolytes, biological cells, and polycrystalline, amorphous, and single-crystal electrically conducting materials. Analysis of such data to provide insight into the detailed, microscopic, physicochemical processes present in the full electrode and bulk material system is a crucial part of IS. Background information on IS and a discussion of its strengths and weaknesses are presented. The use of weighted, complex, nonlinear-least-squares for direct data fitting and for the solution of the ill-posed inversion problem of estimating continuous distributions of activation energies for important response models and for experimental data is illustrated. Replacements for the widely used, but incorrect, complex-electric-modulus data-analysis relations proposed long ago by C. T. Moynihan and associates for disordered ionic conductors, are presented and discussed. Recent proposals for various kinds of universal response behavior are examined and found to be unjustified. The present analysis methods are illustrated by applying them to 24°C data on a lithium aluminosilicate glass and to data over a wide temperature range on single-crystal $CaTiO_3$:30%Al^{3+}.

INTRODUCTION TO IMMITTANCE SPECTROSCOPY

Electrical frequency-response measurements are usually carried out at the impedance or complex-dielectric-constant level. Measurements which involve ionic or defect conduction are typically made at the impedance level, and so the general measurement and analysis approach has come to be called "Impedance Spectroscopy." But impedance, which is an intrinsically complex quantity, is only one of the four connected levels of the more general field of Immittance Spectroscopy. These levels are impedance: $Z(\omega) = Z'(\omega) + iZ''(\omega)$; admittance: $Y(\omega) = [Z(\omega)]^{-1} = Y'(\omega) + iY''(\omega)$; complex dielectric constant (or complex capacitance): $\epsilon(\omega) = Y(\omega)/(i\omega C_C) = \epsilon'(\omega) - i\epsilon''(\omega)$, where C_C is the capacitance of the empty measurement cell; and the complex electrical modulus: $M(\omega) = [\epsilon(\omega)]^{-1}$. Here, $i \equiv \sqrt{-1}$. Also relevant are the related specific quantities, the complex conductivity: $\sigma(\omega) = (i\omega\epsilon_V)\epsilon(\omega) = \sigma'(\omega) + i\sigma''(\omega)$, where ϵ_V is the permittivity of vacuum, and the complex resistivity: $\rho(\omega) = [\sigma(\omega)]^{-1} = \rho'(\omega) + i\rho''(\omega)$. A glossary of acronyms and other definitions appears at the end of this work.

A brief introduction to IS appears in [1], and many details in [2]. In recent years, a great many practical applications of IS have been found [3], such as corrosion analysis, battery testing, characterization of anodized and other films, tooth decay, concrete testing, and even detection of micropores in condoms. Raw measurements, even over a very wide frequency range, are rarely enough, however, and detailed analysis of the data is usually required to elucidate the often complex phenomena involved in the response. The present work is concerned both with methods of analysis and with their results. We may adapt Socrates' dictum: "The unexamined life is not worth living," to the present area as: Inadequately analyzed data are not worth generating!

Mat. Res. Soc. Symp. Proc. Vol. 411 ©1996 Materials Research Society

A crucial procedure in IS analysis is the use of complex nonlinear least squares [CNLS] fitting of data to a model [4-6]. The LEVM CNLS program [4] has been used for the present analyses. CNLS fitting has been shown to have tremendous resolving power [6,7], and it is indispensable in allowing one to resolve the many different processes possibly present and intertwined in measured data, leading to objective estimates of the parameters of the models representing such response, and then, finally, to insight and understanding. Not only can CNLS fitting be used for this purpose, but it also provides a simple way of testing whether data are time-varying or not [8,9], particularly important in corrosion studies, and it allows one to identify and estimate any continuous or discrete distribution of relaxation times [DRT] or distribution of activation energies [DAE] which may be implicit in measured data [7,8,10].

Immittance spectroscopy data analysis allows one to estimate the values of many macroscopic and microscopic properties of the overall material and electrode system. For example, one can, in favorable cases, obtain values for bulk resistivity and dielectric constant, mobile-charge concentrations and mobilities, bulk dissociation and recombination rates, and electrode reaction and adsorption rate constants. Further, when significant bulk dispersion processes are present, they can be identified and analyzed, as illustrated herein.

A potential weakness of IS analysis is the possibility of ambiguity in the choice of an appropriate data fitting model. If this model is made up only of N ideal circuit elements, such as resistors and capacitors, then there are many different connections of these N elements which can lead to exactly the same frequency response over the entire frequency range when the parameter values are properly selected. But usually one of the set of connections is more appropriate physically than the others. It is then necessary to use additional information, such as IS results over a range of temperatures, to allow choice of the best fitting model. A simple example of this ambiguity is presented in Fig. 1 [11].

Many different equivalent circuits have been proposed as models for data fitting when a detailed microscopic model is lacking. Most of them involve distributed circuit elements [DCE], such as transmission lines, as well as ideal elements. An important power-law DCE is the constant-phase element [CPE], $\sigma(\omega) = C(i\omega)^{\gamma}$, where $0 \leq \gamma \leq 1$. The presence of one or more DCE's in an equivalent circuit greatly reduces or removes the ambiguity mentioned above. But there are still instances where two different models can yield essentially identical real- or imaginary-part fits, especially of noisy band-limited data [12-14].

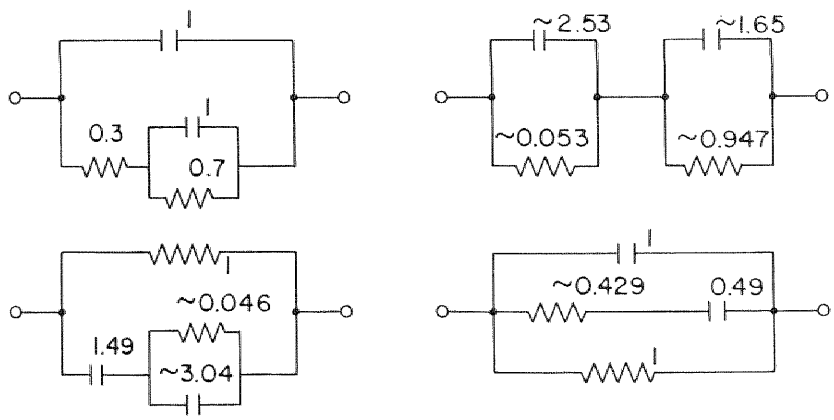

Fig. 1. Four circuits with the same frequency response. Units: Farads and ohms.

It is important to distinguish between response contributions arising from conductive-system dispersion [CSD], which includes a DC path as an intrinsic part of the total response, and dielectric-system dispersion [DSD], which does not. DSD response is associated with ordinary dipolar dielectric behavior and possibly with the localized motion of charges which cannot percolate through the entire material [10,15]. We may represent either type of dispersed response by means of the normalized immittance response function

$$I_k(\Omega_k) \equiv [U_k(\Omega_k) - U_k(\infty)]/[U_k(0) - U_k(\infty)] = I'_k + j\,I''_k, \tag{1}$$

where "k" is taken as "C" for CSD and "D" for DSD. Then, $U_C(\Omega_C) \equiv Z_C(\Omega_C)$, $U_D(\Omega_D) \equiv \epsilon_D{}^*(\Omega_D)$, and $\Omega_k \equiv \omega\tau_k$, where τ_k is a relaxation time associated with the appropriate dispersion model. With these definitions, $I_k(0) = 1$ and $I_k(\infty) = 0$. Here the important quantity $\epsilon'_D(\infty) \equiv \epsilon_{D\infty}$ is the high-frequency dielectric constant associated with the bulk capacitance of the filled measuring cell. An important equivalent circuit for representing CSD, DSD, and possible electrode response is presented in Fig. 2 [16]. Here, $R_\infty = R_{C\infty} \equiv Z'_C(\infty)$ and $C_\infty = C_{D\infty} \equiv \epsilon_{D\infty}C_C$. We may also write $\rho_{C0} \equiv \rho'_C(0)$, and $\sigma_0 \equiv \sigma'(0) = \rho_{C0}^{-1}$. Note that σ_0 and $\sigma_\infty \equiv \sigma'(\infty)$ are intrinsically CSD quantities and need no identifying subscript. Further, let $\Delta\epsilon_k \equiv \epsilon'_k(0) - \epsilon'_k(\infty)$ and $\Delta\sigma'(\omega) \equiv \sigma'(\omega) - \sigma_0$.

It has been known for a long time that nearly all materials exhibiting CSD are thermally activated. Further, σ_0 and τ_C are usually found to have the same or approximately the same activation energies. We may write a typical activated relaxation time as

$$\tau = \tau_a \exp(E/k_BT), \tag{2}$$

where τ_a^{-1} is a barrier attempt frequency, usually larger than $10^{12}\,s^{-1}$, and k_B is the Boltzmann constant. But dispersed response of a thermally activated material can always be represented by a model involving a DAE, and so by an associated DRT. Consider CSD response involving a DAE with $0 \le E \le E_H$. Then we may define

$$\tau_C = \tau_a \exp(E_H/k_BT). \tag{3}$$

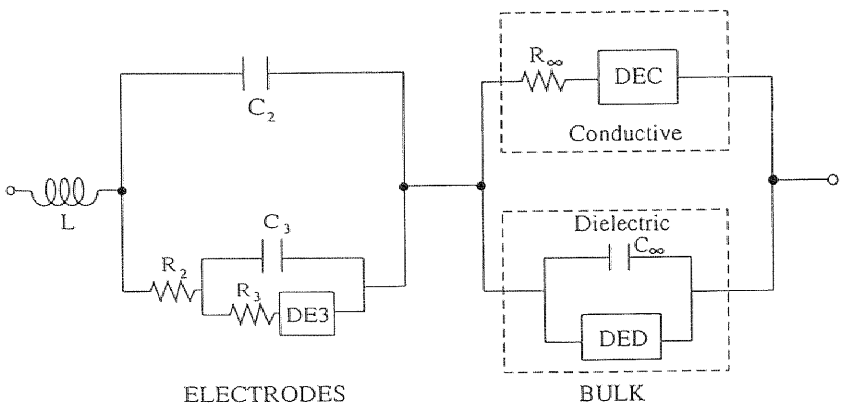

Fig. 2. Equivalent circuit which includes electrode polarization, CSD (i.e., DEC), and DSD (i.e., DED) effects [16]. DE3, DEC, and DED are distributed circuit elements. Not all circuit elements shown need be present and operative.

Let us now write

$$\rho_{C0} = (\tau_a/\epsilon_V K_C)\exp(E_\rho/k_B T), \tag{4}$$

where K_C is a necessarily dimensionless parameter. Consider the situation where τ_C and ρ_{C0} have exactly the same temperature dependence. Then if $E_\rho = E_H$, K_C must be temperature independent, while if $E_\rho \neq E_H$, it must be thermally activated with the energy $E_\rho - E_H$. Even when $E_\rho = E_H$, the temperature dependences of τ_C and ρ_{C0} may differ slightly when K_C is proportional to T^{-1}. Because of inaccuracies in experimental data, it is usually difficult to distinguish between these various possibilities, but a helpful approach is discussed later.

DISTRIBUTIONS AND MODELING EQUATIONS

Estimation of Distributions

For convenience, define $x \equiv \tau/\tau_k$ and $y \equiv ln(x)$. Let $G(x)$ represent a DRT; then since $F(y)|dy| = G(x)|dx|$, it follows that $F(y) = x\,G(x)$ and is proportional to the associated DAE [12,15]. Then one may write in general [7,8,10],

$$I_k(\Omega_k) = \int_0^\infty \frac{G(x)\,dx}{1 + i\,\Omega_k\,x} = \int_{-\infty}^\infty \frac{F(y)dy}{1 + i\,\Omega_k \exp(y)}. \tag{5}$$

Other quantities needed later are the moments of the distribution. They are given by

$$< x^n > \equiv \int_0^\infty x^n G(x)\,dx = \int_{-\infty}^\infty \exp(ny)\,F(y)dy. \tag{6}$$

They are non-zero and finite, at least for $|n| \leq 2$, for physically realizable distributions [10,17]. For properly normalized distributions, $< x^0 > = 1$. Note that $G(x)$, $F(y)$, and $< x^n >$ depend only on the shape of the distribution, not on τ_k directly.

Although the estimation of $F(y)$ for either CSD or DSD is an ill-posed inversion problem when the distribution is intrinsically continuous, it has, nevertheless, been found possible to obtain excellent estimates by using LEVM to fit frequency response data to an appropriate equivalent circuit. For CSD, the circuit is composed of M blocks in series, each block made up of a resistor and capacitor in parallel, while for DSD, the dual of this circuit is used: M blocks in parallel, each made up of a resistor and capacitor in series [7,8,16].

An instructive CSD example is provided by the distribution for the Kohlrausch-Williams-Watts [KWW] fractional-exponential response model [18], which, for a value of the exponent β of 0.5, may be expressed as

$$G(x) = (4\pi x)^{-1/2}\exp(-x/4), \tag{7}$$

or, on transforming to $F(y)$,

$$F(y) = [\exp(y)/4\pi]^{1/2}\exp[-\exp(y)/4]. \tag{8}$$

Figure 3(a) shows results for the inversion of accurate CSD data calculated using Eqs. (5) and (8). For this data set, $\epsilon_{C0} \equiv \epsilon'_C(0) = 20$ and $\epsilon_{D\infty} = 10$, so $\epsilon(0) = 30$ [10]. Here the c_m values are points on the continuous-distribution line. For the bottom curve, inversion was carried out without explicit recognition of the presence of a non-zero value of $\epsilon_{D\infty}$, while the top one incorporated this element as a separate part of the fitting model. The graph shows that the

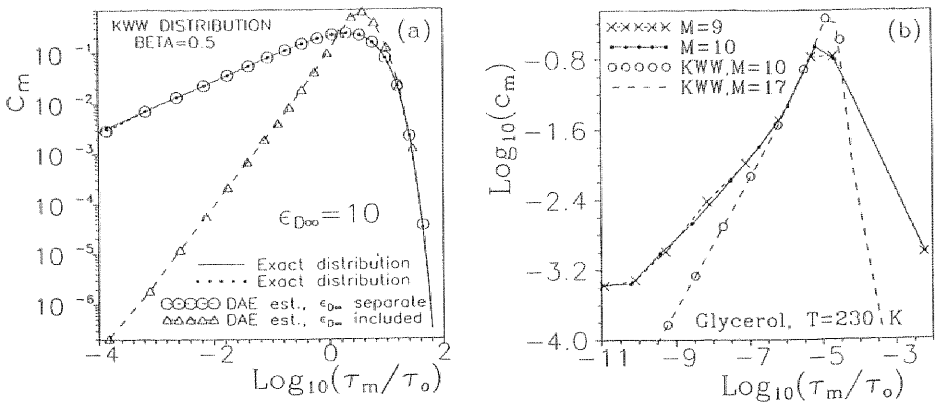

Fig. 3. (a) Distribution estimates for inversion of exact KWW frequency response data. Here and hereafter, $\tau_0 = 1\ s$. (b) Estimates of an unknown continuous distribution associated with glycerol data. The values $\{c_m,\tau_m\}$ $(1 \leq m \leq M)$ specify estimated points on a continuous distribution.

estimated points (circular symbols) for the top curve agree very closely with the true values (since they enclose the exact data points quite evenly) and involve a left-side log-log slope (hereafter just "slope"), s, of 0.5, in agreement with the predictions of Eq. (8). But the limiting slope of the bottom curve is 1.5, properly accounting for the presence of the non-zero $\epsilon_{D\infty}$ but leading to an entirely wrong estimate of $F(y)$.

Figure 3(b) shows inversion results for experimental glycerol DSD data at 230 K. Because of noise in the data, the maximum useful value of M was about 10. For comparison, a KWW distribution with fractional exponent of 0.72 is shown. It was obtained by directly fitting the frequency-response data to the KWW model with weighting that emphasized the peak region of the response, and then estimating the distribution from fit-model data. Clearly, the KWW model represents only part of the response [7]. The LEVM inversion method leads to both high resolution and high discriminatory power because it allows the τ_m's to be free fitting parameters. Fig. 4 shows the inversion of data which involve both a continuous distribution and a single-point discrete distribution. The sharp transitions of the continuous distribution are far better predicted than is possible with other inversion methods, and the discrete point is fully discriminated from the continuous ones. The positions of the latter vary with different M values, but that of the discrete point does not.

Moynihan Relations and Limiting Frequency-Response Equations

In 1972-1973, Moynihan and associates presented some related equations connecting limiting high-frequency and low-frequency results for a material showing CSD [19]. Written in the present notation, these widely used equations are, for the usual condition $\rho'_C(\infty) = 0$,

$$\sigma_0/\epsilon_V = (\epsilon_{D\infty}/\tau_C)/ < x > , \tag{9}$$

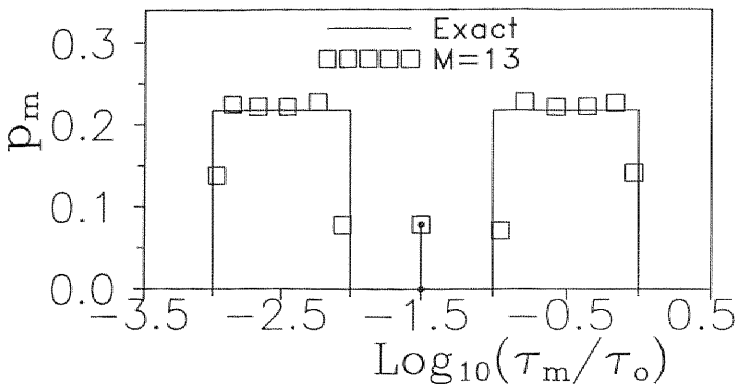

Fig. 4. LEVM inversion results for combined continuous and discrete distributions. The discrete point is that with a solid enclosed dot. Here p_m denotes either c_m or d_m.

$$\sigma_\infty/\epsilon_V = (\epsilon_{D\infty}/\tau_C) < x^{-1} > , \tag{10}$$

and

$$\epsilon_{C0} = \epsilon_{D\infty}[\{ < x^2 > /(< x >)^2\} - 1], \tag{11}$$

where a KWW DRT was usually used for the $G(x)$ of Eq. (6) [19].

Equation (9) indicates that σ_0 and τ_C will have the same activation energy if $\epsilon_{D\infty}$ is independent of temperature and the shape of the distribution is temperature independent, so that $< x >$ does not vary with temperature. But these equations are physically unrealistic because they connect CSD quantities with $\epsilon_{D\infty}$, a purely dielectric response element. One would expect CSD response to be essentially independent of $\epsilon_{D\infty}$, and even for simultaneously present CSD and DSD responses, it should be a good approximation to take their effects independent, as is implicit in the circuit of Fig. 2. Thus, Eqs. (9-11) need to be replaced.

It has been shown elsewhere [8,10] that the Moynihan CSD analysis involves an improper generalization from a situation with a single Maxwell relaxation time to one with a continuous DRT. For an arbitrary, normalized response function, $I(\omega)$, it leads to the following modulus-level response when $\rho'_C(\infty) = 0$,

$$M_{C1}(\omega) = [1 - I(\omega)]/\epsilon_{D\infty}, \tag{12}$$

instead of the standard result $M_{C0}(\omega) \equiv (i\omega\epsilon_V/\sigma_0)I(\omega)$. These expressions are only consistent for a single relaxation time, but when Eq. (12) is corrected by the replacement of $\epsilon_{D\infty}$ by $\epsilon_{C\infty}$ [8, 10], it represents a valid alternative to the use of $M_{C0}(\omega)$ for fitting experimental CSD data.

A recent analysis of a general CSD situation has led to exact relations similar to those of Moynihan and associates but ones which apply for $\rho'_C(\infty) = 0$ or non-zero [10]. In the $\rho'_C(\infty) = 0$ situation, they reduce to

$$\sigma_0/\epsilon_V = (\epsilon_{C0}/\tau_C)/ < x > , \tag{13}$$

$$\sigma_\infty = \sigma_0[< x^{-2} > /(< x^{-1} >)^2], \tag{14}$$

and

$$\epsilon_{C\infty} = \epsilon_{C0}/[< x^{-1} > \ < x >]. \tag{15}$$

Note that only CSD quantities are involved in the above equations; the moments involve a CSD DRT; and Eq. (13) replaces both Eqs. (9) and (11). With the help of one of the Kronig-Kramers relations [8], one can transform Eq. (13) to yield

$$< x > \ = \lim_{\omega \to 0}[- \rho_C'^{\prime}(\omega)/\rho_{C0}\omega\tau_0] = (2/\pi\tau_0)\int_0^\infty [1 - \{\rho_C'(\omega)/\rho_{C0}\}]\omega^{-2}d\omega, \tag{16}$$

Here, no knowledge of $G(x)$ is needed, but a good estimate of ρ_{C0} is required, and accurate evaluation of the integral may require extrapolation beyond the measured ω range. The subscript "C" denotes, as usual, that $\rho_C'(\omega)$ involves only CSD response and must not include electrode and/or DSD contributions. Because of a certain duality between CSD and DSD response functions [12], DSD equations similar to those above also hold exactly. The one of most interest is

$$\rho_{D0} = (\Delta\epsilon_D\tau_D/\epsilon_V\epsilon_{D0}^2) < x > , \tag{17}$$

where here the average is over the DSD distribution, and ρ_{D0} leads to no contribution to σ_0.

It is instructive to consider results for a specific DAE. The simple, symmetric Gaussian DAE will be used for this purpose. It can be expressed in terms of $F(y)$ as [13]

$$F(y) = \pi^{-1/2}\xi^{-1}\exp[- (y/\xi)^2], \tag{18}$$

Here, ξ is a width parameter, and $F(y)$ approaches a δ-function as $\xi \to 0$. Under certain conditions it has been shown that ξ is proportional to T^{-1} [20,21], so the dispersion becomes broader for smaller T, and some of its moments are, for $n = \pm 2$, ± 1, and 0: $\exp(\xi^2)$, $\exp[(\xi/2)^2]$, and 1, respectively [20]. It follows that $\sigma_\infty/\sigma_0 = \epsilon_{C0}/\epsilon_{C\infty} = \exp(\xi^2/2)$, results which have also been verified numerically. Incidentally, it has recently been claimed that a new Coulomb-fluctuation response model [21] yields universal frequency response, but the model has been shown to involve just a Gaussian DAE, as above [20]. It cannot lead to such response both because it involves symmetrical behavior in the frequency domain and because it does not yield finite-length frequency regions with CPE-type fractional power-law response, a truly universal characteristic of nearly all dispersed behavior.

FITTING FREQUENCY-RESPONSE DATA

Lithium Aluminosilicate Glass

For simplicity, it is worthwhile to begin with data which can be well analyzed without the need to include DSD response. The Li_2O-Al_2O_3-$2SiO_2$ [LAS] glass data set, kindly provided by Dr. Moynihan, has been fitted by several investigators since its first publication [19]. Their results [22], as well as those for other similar disordered materials, showed excess loss in the high-frequency region which was not well accounted for by fitting with plausible response models. Such excess loss has been characterized as endemic in the vitreous state [19].

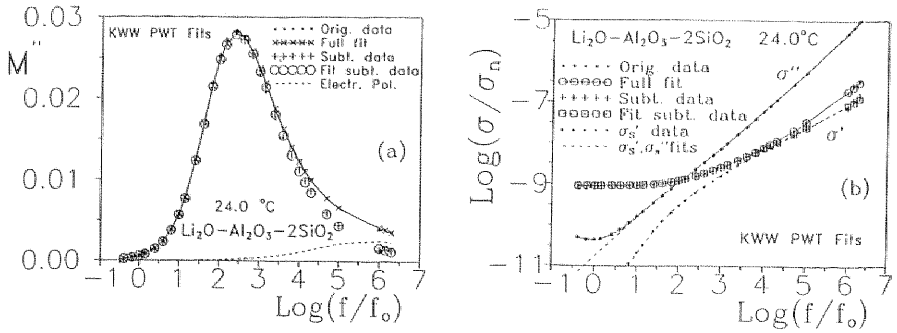

Fig. 5. CNLS fits of lithium aluminosilicate glass data using the KWW model and electrode-polarization circuit elements in series. Here "Subt." denotes subtraction of electrode effects.

The response of the above material has been fitted using an approximate but quite accurate KWW model incorporated in LEVM [10]. It involves the parameters ρ_{C0}, τ_C, and the fractional exponent β. In addition, $\epsilon_{D\infty}$ was also a free fitting parameter, and it was found desirable to account for additional response, almost certainly electrode polarization effects, by means of the parallel combination of a CPE and ideal capacitor, all in series with the KWW CSD response model, as in Fig. 2 [10].

Figure 5 shows the data and M-level fit results for $M''(\omega)$ and $\sigma(\omega)$. In Fig. 5(a), the electrode contribution is also shown separately. A great advantage of CNLS fitting is that once best-fit, objective estimates of the free parameters of the model have been obtained, they may be used to predict the response of the individual parts of the full fitting model. In Fig. 5(a), we see that the data are very well fitted by the full model, and that when electrode effects have been subtracted from the data and the fit model, the excess high-frequency loss is eliminated and the KWW model alone yields an excellent fit of the resultant data.

Similar results appear in Fig. 5(b). The $\sigma_S'{}'$ curve shows the response with the electrode contribution subtracted, and the σ_S' curves involve such subtraction and that of σ_0 as well. We see that electrode effects are most important for $\sigma_S'{}'$ at low frequencies and for σ_S' at high frequencies, contrary to the usual expectation of the dominance of such effects at low frequencies. The limiting slope of σ_S' is β and is about 0.53 here. These fits are much better than previous ones of the same data, particularly ones that used Eq. (12) [22]. But in a recent KWW fit of sodium trisilicate glass data, Nowick and Lim reported poor results [23], ones which possibly arose from the use of the incorrect approach of Eq. (12) rather than proper CSD analysis [8,10].

Al^{3+}-doped Crystalline $CaTiO_3$

Data for this material over the temperature range from 51 K to 626 K were kindly provided by Professor Nowick, who, with his associates, has published several frequency-response analyses for these data and several other disordered materials [24-27]. They suggested that the response of many such materials could be well described by the expression

$$\sigma'(\omega) = \sigma_0 + A\omega^{\gamma} + B\omega^{1}, \tag{19}$$

where A is thermally activated; B involves only small temperature dependence; and $\gamma \simeq 0.6$, independent of temperature [25-27]. The first two terms on the right may be identified as representing CSD and the last as DSD. The last term is an example of the "new" or "second" universal response first proposed by these authors [24], one which corresponds to frequency-independent dielectric loss. Here "first" universality refers to ordinary power-law response, as exemplified by the CPE. A serious problem with the use of Eq. (19) is that it does not lend itself to CNLS analysis, required in order to better separate ambiguous fitting models [10,20]. Thus, more appropriate fully complex CSD and DSD fitting models are needed.

Recent preliminary CNLS analysis of the present data showed that it indeed involved both CSD and DSD contributions [28], but an effective-medium CSD response model which has been claimed to be universal [29] was used. It turned out to be unsatisfactory and non-universal, and therefore the following empirical ZC model [2] has been employed in its place [30],

$$\sigma_{\mathrm{C}}(\omega) = \sigma_0[1 + \{\mathrm{i}\,\omega\tau_{\mathrm{c}}\}^{\gamma}], \tag{20}$$

where $0 \leq \gamma \leq 1$. When one combines Eqs. (3), (4), and (13), it follows that

$$\tau_{\mathrm{c}}\sigma_0/\epsilon_{\mathrm{V}} = \epsilon_{\mathrm{C0}}/ < x > \equiv \epsilon_{\mathrm{C}\tau} = K_{\mathrm{C}}\exp[(E_{\mathrm{H}} - E_{\rho})/k_B T], \tag{21}$$

where $\epsilon_{\mathrm{C}\tau}$ is a new τ-related quantity which usually exhibits much less temperature dependence than does τ_{c} or σ_0. Now Eq. (20) may be rewritten as

$$\sigma_{\mathrm{C}}(\omega) = \sigma_0[1 + \{\mathrm{i}\,\omega\epsilon_{\mathrm{V}}\epsilon_{\mathrm{C}\tau}/\sigma_0\}^{\gamma}], \tag{22}$$

An important virtue of the introduction of $\epsilon_{\mathrm{C}\tau}$ as a fitting parameter in place of τ_{C} is that it provides a sensitive measure of the equality or inequality of E_{H} and E_{ρ} and of possible differences in temperature dependence between σ_0 and τ_{C}. Note that when $E_{\mathrm{H}} = E_{\rho}$ and K_{C} is a constant or proportional to T^{-1}, $\epsilon_{\mathrm{C}\tau}$ will be temperature independent or proportional to T^{-1}. Elliott [31] has characterized a parameter equivalent to K_{C} as containing "information on the (active) carrier concentration, ionic hopping distance, etc" of ionic glasses. Equation (21) connects K_{C} explicitly to measurable quantities of the overall CSD response.

In the earlier analysis of the some of the present data [28], the use of an exponential DAE, leading to $I_{EDAE}(\omega)$, was found satisfactory for the DSD part of the response. It involves a parameter ϕ which satisfies $-\infty < \phi < \infty$, and $1 - \phi$ is equal to the slope of the $\sigma'(\omega)$, or, more properly, the $\Delta\sigma'(\omega)$ response, for $|\phi| \leq 0.5$. When $\phi = 0$, the DAE reduces to that of a flat-top box from $0 \leq E \leq E_H$ [10, 12, 13]. The DSD part of the response may be written as

$$\epsilon_{\mathrm{D}}(\omega) = \sigma_{\mathrm{D}}(\omega)/i\omega\epsilon_V = \epsilon_{\mathrm{D}\infty} + \Delta\epsilon_{\mathrm{D}} I_{EDAE}(\Omega_{\mathrm{D}}), \tag{23}$$

where $\Omega_{\mathrm{D}} \equiv \omega\tau_{\rho}$ and $I_{EDAE}(\omega)$ is only defined in quadrature form for arbitrary ϕ but is included as a DCE in LEVM.. The full response model, including a possible electrode-polarization contribution, $\sigma_{\mathrm{el}}(\omega)$, is

$$\sigma(\omega) = \sigma_{\mathrm{B}}(\omega)/[1 + \{\sigma_{\mathrm{B}}(\omega)/\sigma_{\mathrm{el}}(\omega)\}], \tag{24}$$

where $\sigma_{\mathrm{B}}(\omega) \equiv \sigma_{\mathrm{C}}(\omega) + \sigma_{\mathrm{D}}(\omega)$.

Figure 6(a) compares two different estimates of the slopes of the present $\Delta\sigma'(\omega)$ data. The solid-circle ones [25,27] were probably mostly or entirely obtained graphically, while the open-square points are the results of NLS fitting of the Eq.-(23) model to $\epsilon''(\omega)$ data at low

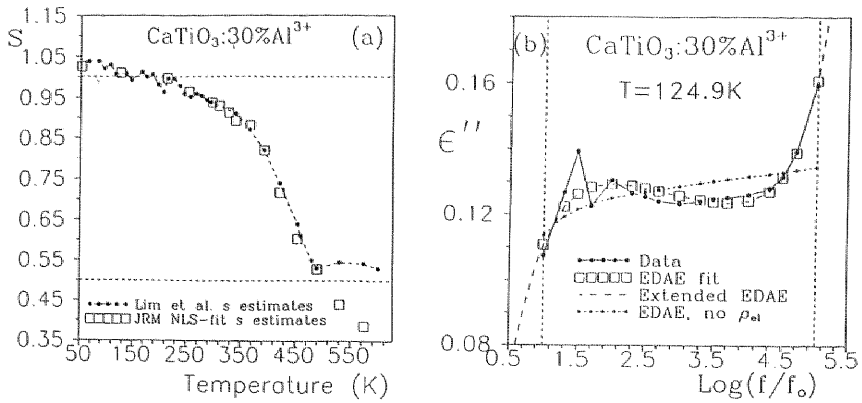

Fig. 6. (a) Temperature dependence of two different estimates of the log-log slope of $[\sigma'(\omega) - \sigma_0]$ data. (b) Frequency dependence of typical low-temperature $\epsilon''(\omega)$ data and fits.

temperatures where σ_0 was negligible, or of the Eq.-(22) model to $\sigma'(\omega)$ data at higher temperatures. The difference between the results at the highest temperatures arises from electrode effects and is discussed below. Before considering the possibility of using Eqs. (22)-(24) to try to take account of different processes which may be present, it is worthwhile to look at some of the data themselves.

Figure 6(b) shows the $\epsilon''(\omega)$ data available at 124.9 K. Besides the large noise at low frequencies, an appreciable increase in loss is apparent at the high-frequency end; certainly the data do not indicate a close approach to constant loss. CNLS fitting results using Eq. (23) are shown with and without the presence in the model of a series electrode resistivity ρ_{el}. Without separate account of ρ_{el}, the high-frequency limiting slope is about 1.01, as in Fig. 6(a), while it is reduced to about 0.98 when the effect of ρ_{el} is properly accounted for. These results do not indicate the presence of a "second universality," but they explain the reason for the $s > 1$ values in Fig. 6(a), an effect which disappears when detailed analysis is carried out [30].

Figure 7(a) shows the frequency response and CNLS fit results for the highest available temperature. Good fits of the high-temperature data sets were obtained with an electrode contribution represented by a CPE and an ideal capacitance in parallel, just as in the LAS glass analysis. But a slightly improved fit was found for the present temperature when a series ρ_{el} was also allowed to be present. Both the $\sigma'(\omega)$ and $\sigma''(\omega)$ fits are exceptionally good, although electrode polarization evidently plays a dominant role over much of the range. The figure shows the $\sigma'_C(\omega)$ and $\sigma''_C(\omega)$ responses with electrode effects removed and the further result of subtracting the effects of σ_0 as well. It is clear that the extent of the available high-frequency data is insufficient to yield an accurate estimate of γ for this temperature.

The most important results of the CNLS analysis of the present data are shown in Fig. 7(b). Although it is plausible to expect that the CSD and DSD responses extend over the entire temperature range, toward the ends of the present range one or the other of these responses becomes too small to be resolved by the fitting procedure, and the accuracy of the slope estimates for the smaller response suffers as one approaches such regions. Further, as discussed above, the estimates of the CSD slope, γ, become uncertain when most of the response is dominated by

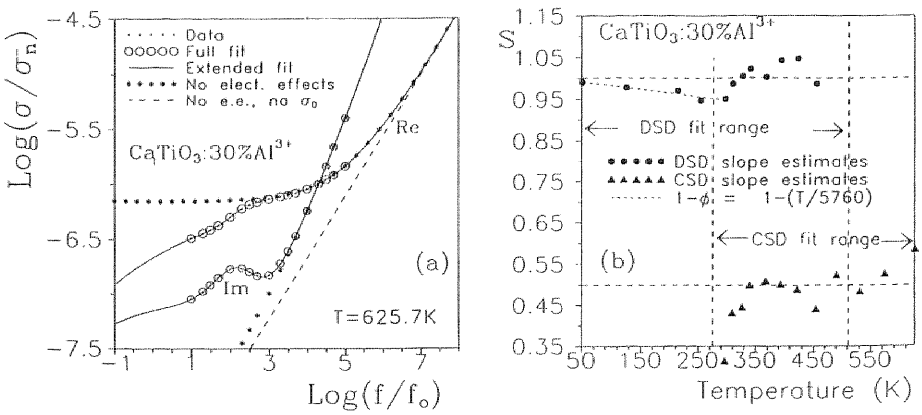

Fig. 7. (a) Frequency dependence of σ' for the highest-temperature data available. (b) CNLS estimates of the temperature dependences of the slopes of separate DSD and CSD processes.

σ_0. Nevertheless, comparison of the two highest-temperature CSD slope estimates in Figs. 6(a) and 7(b) shows that their small values in Fig. 6(a) arise from not accounting for electrode effects. Incidentally, Nowick and associates assumed *ab initio* that the DSD slope was unity and temperature independent, and they quote only a temperature independent value of the CSD slope of 0.55 [27].

The CSD part of the fitting led to nearly constant $\epsilon_{C\tau}$ estimates over the higher temperature part of the range where σ_0(T) could be best estimated. $\epsilon_{C\tau}$ showed no activated behavior and varied approximately randomly around an average of 36, strong evidence that $E_H = E_\rho$ [30]. Then Eq. (21) shows that $K_C \simeq 36$. When this value is combined with the estimate of τ_a/K_C obtained from direct Eq. (4) NLS fitting of ρ_{C0}(T) data, the estimate $\tau_a \simeq 4.0\text{x}10^{-15}s$ is obtained. In addition, the fit yielded $E_H = E_\rho \simeq 1.13$ eV, surprisingly smaller than the estimates of 1.22 and 1.25 eV found by Nowick and associates for E_ρ and E_H, respectively [27]. Incidentally, when K_C was set to E_H/k_BT, as suggested in [32], estimates of $\tau_a \simeq 1.1\text{x}10^{-15}s$ and $E_H = E_\rho \simeq 1.17$ eV were found. The most significant estimates of γ cluster near 0.5, suggesting that the response is associated with diffusion. The use of a finite-length Warburg diffusion model [2] led, however, to far worse fits than did Eq. (22) [30].

CNLS fitting led to an approximately constant estimate for ϵ_{C0} of about 60 and to approximate temperature independence of the $\Delta\epsilon_D$ of Eq. (23). One would not expect it to be thermally activated, but the EDAE model used for DSD fitting assumes that τ_D is activated. It was found to vary too irregularly to allow a significant estimate of its activation energy to be obtained [30]. But one of the characteristic features of the thermally-activated EDAE model of dielectric dispersion is that it predicts that ϕ be proportional to T [12,15]. We see from Fig. 7(b) that over a wide low-temperature range the DSD slope, $1-\phi$, well satisfies this requirement. It is likely that the larger DSD s values at higher temperatures, where the DSD response becomes a smaller and smaller part of the total, cannot be estimated accurately enough to show the continuation of this behavior. In any event, the agreement with the theoretical slope dependence

at lower temperatures strongly suggests that the "second universality" proposed by Nowick and associates fails to apply for this material over a wide temperature range.

GLOSSARY OF PRINCIPAL ACRONYMS AND SYMBOLS

C	Subscript denoting conductive
c_m, d_m, p_m	Strength coefficients for distributions which are continuous, discrete, or both
CNLS	Complex nonlinear least squares
CPE	Constant-phase distributed circuit element
CSD	Conductive-system dispersion
D	Subscript denoting dielectric
DAE	Distribution of activation energies
DCE	Distributed circuit elment, such as the CPE
DRT	Distribution of relaxation times
DSD	Dielectric-system dispersion
EDAE	Exponential distribution of activation energies
ϵ_{Cr}	Important effective dielectric quantity defined in Eq. (21)
ϵ_V	Permittivity of vacuum, 8.8542×10^{-12} Fm^{-1}
LAS	Li_2O-Al_2O_3-$2SiO_2$ glass
LEVM	The CNLS fitting program used herein
M	The number of RC blocks used for inversion of frequency-response data
NLS	Nonlinear least squares
ϕ	A slope-related parameter of the EDAE model, here applied for DSD response
s	Log-log slope; either direct or average value from power-law exponent fit
ZC	Cole-Cole DSD response model used at the impedance level for CSD response

REFERENCES

1. J. R. Macdonald, Ann. Biomed. Eng. **20** (1992) 289.
2. J. R. Macdonald, editor, Impedance Spectroscopy – Emphasizing Solid Materials and Systems (Wiley-Interscience, New York, 1987).
3. See the papers presented at the Second International Symposium on Electrochemical Impedance Spectroscopy, Electrochim. Acta **38** (1993) 1799-2133.
4. J. R. Macdonald and L. D. Potter, Jr., Solid State Ionics **23** (1987) 61. The latest version of the LEVM fitting program may be obtained from Solartron Instruments, Farnborough, England, Attn. Brian Sayers, +44 (0) 1252 376 666, e-mail: 100444.3217@compuserve.com.
5. B. A. Boukamp, Solid State Ionics **18/19** (1986); **20** (1986) 31.
6. J. R. Macdonald, J. Electroanal. Chem. **307** (1991) 1.
7. J. R. Macdonald, J. Chem. Phys. **102** (1995) 6241.
8. B. A. Boukamp and J. R. Macdonald, Solid State Ionics **74** (1994) 85.

9. B. A. Boukamp, J. Electrochem. Soc. **142** (1995) 1885.
10. J. R. Macdonald, J. Non-Cryst. Solids, to be published in May 1996.
11. J. R. Macdonald, Electrochim. Acta **35** (1990) 1483.
12. J. R. Macdonald, J. Appl. Phys. **58** (1985) 1955,1971.
13. J. R. Macdonald, J. Appl. Phys. **61** (1987) 700
14. J. R. Macdonald, J. Appl. Phys. **62** (1987) R51. The KWW distribution is misidentified here as a stable Lévy distribution; instead it is the characteristic function of such a distribution.
15. J. R. Macdonald and J. C. Wang, Solid State Ionics **60** (1993) 319; J. R. Macdonald, J. Chem. Phys. **36** (1962) 345.
16. J. R. Macdonald, J. Electroanal. Chem. **378** (1994) 17. Replace "relation" by "relaxation" in title.
17. J. R. Macdonald, Solid State Ionics **25** (1987) 271.
18. R. Kohlrausch, Pogg. Ann. der Phys. und Chemie, (2) **91** (1854) 179; G. Williams and D. C. Watts, Trans. Faraday Soc. **66** (1970) 80.
19. P. B. Macedo, C. T. Moynihan, and R. Bose, Phys. Chem. Glasses **13** (1972) 171; C. T. Moynihan, L. P. Boesch, and N. L. Laberge, ibid **14** (1973) 122.
20. J. R. Macdonald, submitted to Phys. Lett. A.
21. V. N. Bondarev and P. V. Pikhitsa, Phys. Lett. A **196** (1994) 247.
22. C. T. Moynihan, J. Non-Cryst. Solids, **172-174** (1994) 1395.
23. A. S. Nowick and B. S. Lim, J. Non-Cryst. Solids **172-174** (1994) 1389.
24. W. K. Lee, J. F. Liu, and A. S. Nowick, Phys. Rev. Lett. **67** (1991) 1559.
25. B. S. Lim, A. V. Vaysleyb, and A. S. Nowick, Appl. Phys. A **56** (1993) 8.
26. A. S. Nowick, A. V. Vaysleyb, and B. S. Lim, J. Appl. Phys. **76** (1994) 4429.
27. A. S. Nowick, B. S. Lim, and A. V. Vaysleyb, J. Non-Cryst. Solids **172-174** (1994) 1243.
28. J. R. Macdonald, Appl. Phys. A **59** (1994) 181.
29. J. C. Dyre, Phys. Rev. B **48** (1993) 12511.
30. J. R. Macdonald, submitted to J. Non-Cryst. Solids.
31. S. R. Elliott, Solid State Ionics **27**(1988) 131.
32. J. R. Macdonald, Phys. Rev. B **49** (1994-II) 9428.